Journal of Engineering Mathematics **49:** 217–232, 2004.

Fast-converging series for heat conduction in the circular cylinder

KEVIN D. COLE
Mechanical Engineering Dept., University of Nebraska, Lincoln, NE 68588-0656, U.S.A.
E-mail: kcole1@unl.edu

Received 5 November 2003; accepted in revised form 6 April 2004

Abstract. Steady heat conduction in the finite, right-circular cylinder is treated with the method of Green's functions for a variety of boundary conditions. Three forms of the series for the Green's function are discussed: a triple-sum series obtained from eigenfunction expansions; an alternate triple-sum series with improved series convergence found with the method of time partitioning; and, a double-sum series. Influence functions appropriate for the boundary-element method are constructed with the Green's functions to describe a cylinder heated by a specified heat flux over a portion of one face. Numerical examples are given.

Key words: cylinder, Green's functions, Laplace equation, series convergence, time partitioning

1. Introduction

The method of Green's functions (GF) applies to linear differential equations that describe a wide variety of physical phenomena, including heat conduction, fluid flow, and electrochemical potential. In this method the boundary-value problem for the temperature is restated into an integral expression that involves the known boundary conditions and the GF. If the GF is known and if the integral expressions can be evaluated; then the method of GF is a powerful tool for solving many different problems. This paper applies the method of GF to evaluate steady-state temperature in the solid cylinder. One motivation for the work is to find influence functions for boundary-element solutions in the cylinder.

The pertinent literature is summarized next. Several books give a good overview of the GF method such as Morse and Feshbach [1], Carslaw and Jaeger [2], Stakgold [3], and Duffy [4]. Barton [5] carefully discusses the properties of the Dirac delta function and describes the pseudo GF for the Neumann boundary condition. Two books by Butkovskii [6, 7] contain many GF organized according to the type of differential equation. The differential equations are categorized according to a number system for the number of spatial dimensions, the order of the highest time derivative, and the order of the highest spatial derivative. Although Butkovskii's number system clearly distinguishes different equations, there are no subdivisions for the various coordinate systems and boundary conditions. Beck *et al.* [8] give extensive tables of GF for heat conduction and diffusion. The GF are organized with a number system for the number of spatial dimensions, the type of coordinate system, and the type of boundary conditions. Most of the book is devoted to transient heat conduction and few steady GF are given.

Dolgova and Melnikov [9] discuss steady two-dimensional heat conduction in Cartesian and cylindrical coordinates. Fourier-series expansions along one coordinate direction are used to produce single-sum series for the GF. Three examples of GF for the cylinder are given. Most importantly, the slowly-converging portions of the series for the GF are identified and

replaced with closed-form expressions. This approach has been extended and expanded in two recent books by Melnikov [10, 11] to improve the numerical convergence of GF for a variety of equations, coordinate systems, and geometries. The chapters on Laplace and Helmholtz equations include sections on the cylinder, and several GF are given. Although wide-ranging, the improvement of convergence is applied only to GF.

Previous work by the author for steady heat conduction in the rectangle [12] and the infinite strip [13] provide a variety of GF with boundary conditions of type 1, 2 or 3. The GF are organized and identified by Beck's numbering system. In previous work with the parallelepiped [14], double-sum GF are given that are numerically better behaved than the classic triple-sum GF developed from eigenfunction expansions. Temperature expressions based on these GF also have improved convergence from the replacement of intransigent summations by fully-summed forms.

This paper is an extension of previous work with Cartesian geometries to the cylinder. The contribution of the present paper is threefold. First, several GF for the solid cylinder are given in double-sum form which are numerically better behaved than the classic triple-sum GF. Second, an alternate triple-sum GF is derived using time partitioning, a general-purpose method to improve the convergence of steady GF. Third, integrals are carried out to produce series expressions for temperature caused by small heated regions on the boundaries, which have application as influence functions for boundary-element methods. The work encompasses twenty-seven solid-cylinder geometries containing any combination of boundaries of types 1, 2, and 3.

2. Temperature problem

Consider the steady temperature in the cylinder caused either by heating at the boundaries or by internal energy generation. The temperature satisfies

$$\frac{\partial^2 T}{\partial r^2} + \frac{1}{r}\frac{\partial T}{\partial r} + \frac{1}{r^2}\frac{\partial^2 T}{\partial \phi^2} + \frac{\partial^2 T}{\partial z^2} = -\frac{g(r,\phi,z)}{k} \qquad (1)$$

$$0 < z < L;\ 0 \le r < a;\ 0 \le \phi \le 2\pi$$

$$k_i \frac{\partial T}{\partial n_i} + h_i T = f_i \quad \text{for boundaries } i = 1, 2, \text{ or } 3.$$

Here n_i is the outward normal on each surface of the cylinder (at $r = a$, $z = 0$, and $z = L$). The boundary condition represents one of three types at each surface: type 1 for $k_i = 0$, $h_i = 1$, and f_i a specified temperature; type 2 for $k_i = k$, $h_i = 0$, and f_i a specified heat flux; and, type 3 for $k_i = k$ and $f_i = h_i T_\infty$ for convection to surroundings at temperature T_∞. Heat transfer coefficient h_i must be uniform on the i^{th} boundary.

The temperature can be stated in the form of integrals with the method of Green's functions. If the Green's function G is known, the temperature that satisfies Equation (1) is given by:

$$T(r,\phi,z) = \int_{z'=0}^{L}\int_{\phi'=0}^{2\pi}\int_{r'=0}^{a} \frac{g(r',\phi',z')}{k} G(r,\phi,z \mid r',\phi',z')\, r'\mathrm{d}\phi'\mathrm{d}r'\mathrm{d}z'$$

(for volume energy generation)

$$+\sum_{j=1}^{3}\int_{s_j}\frac{f_j}{k}G(r,\phi,z\mid r'_j,\phi'_j,z'_j)\mathrm{d}s'_j$$

(for boundary conditions of type 2 and 3)

$$-\sum_{i=1}^{3}\int_{s_i}f_i\frac{\partial G(r,\phi,z\mid r'_i,\phi'_i,z'_i)}{\partial n'_i}\mathrm{d}s'_i \tag{2}$$

(for boundary conditions of type 1 only).

The same Green's function appears in each integral but is evaluated at locations appropriate for each integral. Here position (r'_i,ϕ'_i,z'_i) is located on surface s_i. The two summations represent all possible combinations of boundary conditions, but with only one type of boundary condition on each of three surfaces of the cylinder. Mixed-type boundary conditions are not treated.

3. Definition of the GF

The steady Green's function represents the response at point (r,ϕ,z) caused by a point source of heat located at (r',ϕ',z'). The GF associated with equation (1) is given by:

$$\begin{aligned}\frac{\partial^2 G}{\partial r^2}+\frac{1}{r}\frac{\partial G}{\partial r}+\frac{1}{r^2}\frac{\partial^2 G}{\partial\phi^2}+\frac{\partial^2 G}{\partial z^2} &= -\frac{1}{r}\delta(r-r')\delta(\phi-\phi')\delta(z-z'), \\ &\qquad 0\le r<a;\ 0\le\phi\le 2\pi;\ 0<z<L, \\ k_i\frac{\partial G}{\partial n_i}+h_i G &= 0 \ \text{ for faces } i=1,2,\ \text{or } 3.\end{aligned} \tag{3}$$

Note that the boundary conditions are homogeneous and of the same type as the temperature problem of Equation (1). The volume energy generation is replaced by point heat source described by a Dirac delta function, δ. Most of the quantities in this discussion have units: $k=[\mathrm{W/m/K}]$; $h=[\mathrm{W/m^2/K}]$; and, $G=[1/\mathrm{m}]$ for steady heat conduction in the cylinder.

4. GF number

We use a number system to keep track of the different possible combinations of boundary conditions and the GF associated with them. A specific GF is identified by a "number" of the form R0JΦ00ZKL in which R, Φ and Z represent the coordinate axes, and the letters following each axis name take on values 1, 2, or 3 to represent the type of boundary conditions present at the body faces normal to that axis. Number 0 is also used to denote the lack of a physical boundary. For example, number R02 represents a solid cylinder (no physical boundary at $r=0$) and with a boundary condition of type 2 at $r=a$. As another example, number R01Φ00Z13 describes a GF for a solid cylinder with the following boundary information: no physical boundary at $r=0$; the curved face at $r=a$ has a type 1 boundary ($G=0$); no physical boundary along angular coordinate ϕ (periodic boundary condition at $\phi=0$ and $\phi=2\pi$); the face at $z=0$ has a type 1 boundary; and, the $z=L$ face has a type 3 boundary (convection). See [8, Chapter 2], for additional details of the number system.

Table 1. Eigenfunctions and norm for solid cylinders. Note $B_2 = ha/k$.

Case	Condition at $r = a$	R_{nm}	$(N_r)^{-1}$ for $n \neq 0$	$(N_r)^{-1}$ for $n = 0$
R01	$R_{nm} = 0$	$J_n(\beta_{nm} r)$	$\frac{2}{a^2 J_n'(\beta_{nm} a)}$	see $n \neq 0$
R02	$\frac{\mathrm{d}R_{nm}}{\mathrm{d}r} = 0$	$J_n(\beta_{nm} r)$	$\frac{2}{a^2 J_n^2(\beta_{nm} a)} \frac{a^2\beta_{nm}^2}{(a^2\beta_{nm}^2 - n^2)}$	$\frac{2}{a^2}$
R03	$k\frac{\mathrm{d}R_{nm}}{\mathrm{d}r} + hR_{nm} = 0$	$J_n(\beta_{nm} r)$	$\frac{2}{a^2 J_n^2(\beta_{nm} a)} \frac{a^2\beta_{nm}^2}{(B_2^2 + a^2\beta_{nm}^2 - n^2)}$	see $n \neq 0$

5. Double-summation form of the GF

The GF stated below contains a double summation with eigenfunctions R_{nm} norms $N_r^{1/2}$ and $N_\phi^{1/2}$, eigenvalues β_{nm} and kernel function P_{nm}, as follows:

$$G(r, \phi, z \mid r', \phi', z') = \frac{P_{00}(z, z')}{N_r(00) N_\phi(0)} + \sum_{m=1}^{\infty} \frac{R_{0m}(r) R_{0m}(r')}{N_r(0m)} \frac{1}{N_\phi(0)} P_{0m}(z, z') + \sum_{n=1}^{\infty} \sum_{m=1}^{\infty} \frac{R_{nm}(r) R_{nm}(r')}{N_r(nm)} \frac{\cos[n(\phi - \phi')]}{N_\phi(n)} P_{nm}(z, z'). \tag{4}$$

The norms associated with the angular direction ϕ are given by $N_\phi(0) = 2\pi$ and $N_\phi(n \neq 0) = \pi$. Each of the three terms in the above equation have physical significance. The first term is proportional to the one-dimensional Green's function along the z-direction, and it is needed only when $\beta_{nm} = 0$ is an eigenvalue (associated with a boundary of type 2 at $r = a$). The second term is proportional to the two-dimensional Green's function in the cylinder described by (r, z) coordinates (no ϕ-dependence), and the third term is the correction for the angle-(ϕ) dependence.

5.1. Eigenfunction R

The r-direction eigenfunction R_{nm} satisfies the following ordinary differential equation

$$R_{nm}'' + \frac{1}{r} R_{nm}' + (\beta_{nm}^2 - \frac{n^2}{r^2}) R_{nm} = 0, \tag{5}$$

where β_{nm} are the associated eigenvalues. (Strictly speaking, the eigenvalues are β_{nm}^2, which can be shown to be real and non-negative. Without ambiguity we take the non-negative square root of β_{nm}^2 and shall refer to them as the "associated eigenvalues" for brevity.) There are three different boundary conditions R0J (J = 1,2, or 3). Eigenfunctions $R_{nm}(r)$ and corresponding norm $N_r(nm)$ are given in Table 1, and Table 2 contains the associated eigenconditions for the solid cylinder.

Table 2. Eigenconditions for solid cylinders.

Case	Eigencondition
R01	$J_n(\beta_{nm}a) = 0$
R02	$J_n'(\beta_{nm}a) = 0$
R03	$\beta_{nm}aJ_n'(\beta_{nm}a) + B_2J_n(\beta_{nm}a) = 0$

5.2. KERNEL FUNCTION P

The kernel function $P_{nm}(z, z')$ must satisfy

$$\frac{\mathrm{d}^2P_{nm}}{\mathrm{d}z^2} - \beta_{nm}^2P_{nm} = -\delta(z - z'), \tag{6}$$

where β_{nm} is the eigenvalue associated with eigenfunction R_{nm}. The kernel function, suppressing the nm subscript, may be written as [14]

$$\begin{aligned} P(z, z') &= \frac{S_2^-(S_1^-\mathrm{e}^{-\beta(2L_i-|z-z'|)} + S_1^+\mathrm{e}^{-\beta(2L_i-z-z')})}{2\beta(S_1^+S_2^+ - S_1^-S_2^-\mathrm{e}^{-2\beta L_i})} \\ &+ \frac{S_2^+(S_1^+\mathrm{e}^{-\beta(|z-z'|)} + S_1^-\mathrm{e}^{-\beta(z+z')})}{2\beta(S_1^+S_2^+ - S_1^-S_2^-\mathrm{e}^{-2\beta L_i})}, \end{aligned} \tag{7}$$

where the subscripts 1 and 2 indicate sides $z = 0$ and $z = L$ of the cylinder, respectively. Parameters S_M^+ and S_M^- depend on the boundary conditions on side M and are given by

$$S_M^+ = \begin{cases} 1 & \text{if side } M \text{ is type 1 or type 2} \\ \beta L + B_M & \text{if side } M \text{ is type 3} \end{cases}, \tag{8}$$

$$S_M^- = \begin{cases} -1 & \text{if side } M \text{ is type 1} \\ 1 & \text{if side } M \text{ is type 2} \\ \beta L - B_M & \text{if side } M \text{ is type 3.} \end{cases} \tag{9}$$

Here $B_M = Lh_M/k$ is the Biot Number for side M, and k is the conductivity of the cylinder. Note that the kernel functions given above contain exponentials, all of which have negative arguments containing eigenvalue β. Since β increases in the series for the GF, these exponentials provide for rapid convergence of the double-sum GF.

The expression for P in Equation (7) is symmetric if z and z' are interchanged and covers several combinations of boundary conditions provided $\beta \neq 0$. The special case of $\beta = 0$ is discussed below.

5.3. KERNEL FUNCTION WITH $\beta = 0$

If the $r = a$ boundary of the cylinder is of type 2, the zero eigenvalue exists. In this case the kernel function must satisfy

$$\frac{\mathrm{d}^2P_{00}}{\mathrm{d}z^2} = -\delta(z - z'), \tag{10}$$

Table 3. Kernel function for $\beta = 0$. Note $B_1 = h_1 L/k$; $B_2 = h_2 L/k$.

Case	$P_{00}(z, z')$ for $z > z'$. (Use $P_{00}(z', z)$ for $z < z'$.)
Z11	$z'(1 - z/L)$
Z12	z'
Z13	$z'[1 - B_2(z/L)/(1 + B_2)]$
Z21	$L - z$
Z22[a]	$((z')^2 + z^2)/(2L) - z + L/3$
Z23	$L(1 + 1/B_2 - z/L)$
Z31	$(B_1 z' - B_1 z' z/L + L - z)/(1 + B_1)$
Z32	$L(1/B_1 + z'/L)$
Z33	$\left(B_1 B_2 z' + B_1 z' - B_1 B_2 z' z/L - B_2 z + B_2 L + L\right)$ $\div (B_1 B_2 + B_1 + B_2)$

[a] See Appendix A for a discussion of the modified GF.

as well as the boundary conditions at $z = 0$ and $z = L$. Since there are nine combinations of boundary conditions (type 1, 2, or 3 at $z = 0$ and $z = L$), there are nine kernel functions P_{00} which are given in Table 3.

A very special condition occurs if the cylinder's *entire* boundary is of type 2, that is, case R02Φ00Z22. In this case strictly speaking the GF as defined in Equation (3) does not exist, and a modified GF must be used instead. A discussion of the modified GF is given in Appendix A.

6. Triple-summation form of the GF

In this section the triple-sum form of the steady GF will be found from the transient GF. The steady GF is found from the transient GF by integration, that is

$$G_{\text{steady}} = \lim_{t\to\infty} \alpha \int_{\tau=0}^{t} G_{\text{transient}}\, \mathrm{d}\tau. \tag{11}$$

Physically, this integral represents a suddenly-appearing heat source maintained steadily for a long time. The transient three-dimensional GF may be assembled as a product of lower-dimension GF according to [8, p. 103]

$$G(r, \phi, z, t\,|r', \phi', z', \tau) = G(r, \phi, t\,|r', \phi', \tau) \times G(z, t\,|z', \tau). \tag{12}$$

These transient GF are well known (see for example [8, Appendix R and Appendix X]) and are given by

$$\begin{aligned} G(r, \phi, t\,|r', \phi', \tau) \;=\; & \frac{R_{00}(r) R_{00}(r')}{N_r(00) N_\phi(0)} \\ & + \sum_{m=1}^{\infty} \mathrm{e}^{-\beta_{nm}^2 \alpha (t-\tau)} \frac{R_{0m}(r) R_{0m}(r')}{N_r(0m)} \frac{1}{N_\phi(0)} \\ & + \sum_{n=1}^{\infty} \sum_{m=1}^{\infty} \mathrm{e}^{-\beta_{nm}^2 \alpha (t-\tau)} \frac{R_{nm}(r) R_{nm}(r')}{N_r(nm)} \frac{\cos[n(\phi - \phi')]}{N_\phi(n)}, \end{aligned} \tag{13}$$

$$G(z, t\,|z', \tau) \;=\; \frac{1}{N_z(0)} + \sum_{\ell=1}^{\infty} \mathrm{e}^{-\lambda_\ell^2 \alpha (t-\tau)} \frac{Z_\ell(z)\, Z_\ell(z')}{N_z(\ell)}. \tag{14}$$

Quantities R_{nm}, N_r, and N_ϕ are the same as discussed earlier associated with the double-sum GF in Equation (4). Eigenfunctions Z_ℓ and norm $N_z(\ell)$ are discussed in the following section. Then multiply the two transient GF together and integrate according to Equation (11) to obtain the steady triple-sum GF:

$$\begin{aligned} G(r, \phi, z\,|r', \phi', z') \;=\; & \frac{R_{00}(r) R_{00}(r')}{N_r(00) N_\phi(0)} \sum_{\ell=1}^{\infty} \frac{1}{\lambda_\ell^2} \frac{Z_\ell(z)\, Z_\ell(z')}{N_z(\ell)} \\ & + \frac{1}{N_\phi(0)} \sum_{m=1}^{\infty} \sum_{\ell=1}^{\infty} \frac{1}{(\beta_{nm}^2 + \lambda_\ell^2)} \frac{R_{0m}(r) R_{0m}(r')}{N_r(0m)} \frac{Z_\ell(z)\, Z_\ell(z')}{N_z(\ell)} \\ & + \sum_{n=1}^{\infty} \sum_{m=1}^{\infty} \sum_{\ell=1}^{\infty} \frac{1}{(\beta_{nm}^2 + \lambda_\ell^2)} \frac{R_{nm}(r) R_{nm}(r')}{N_r(nm)} \\ & \times \frac{\cos[n(\phi - \phi')]}{N_\phi(n)} \frac{Z_\ell(z)\, Z_\ell(z')}{N_z(\ell)}. \end{aligned} \tag{15}$$

The above expression does not include case R02Φ00Z22. Note that the triple-sum GF does not contain any kernel functions (with their convergence-improving exponentials). Consequently the triple-sum GF tends to converge less rapidly than the double-sum GF.

6.1. Eigenfunctions Z_ℓ

The eigenfunctions in Equation (14), $Z_\ell(z)$, satisfy the ordinary differential equations

$$Z_\ell''(z) + \lambda_\ell^2 Z_\ell(z) = 0, \tag{16}$$

where λ_ℓ are the eigenvalues. The boundary conditions are the same as those satisfied by the GF at $z = 0$ and $z = L$. There are nine possible different eigenfunctions depending on the type of boundary conditions on the faces perpendicular to the direction z. These eigenfunctions have been discussed previously [12, 13] and they are given along with their norms and their eigenvalues (or eigenconditions) in Table 4.

6.2. Time partitioning to improve convergence

The triple-sum form of the GF given above converges so slowly as to be impractical for generating numerical results. In this section the method of time partitioning [8, 15] is used to improve the convergence speed.

Time partitioning involves splitting Equation (11) into two terms. Let $u = t - \tau$; then write Equation (11) as

$$G_{\text{steady}} = \alpha \int_{u=0}^{t_1} G_1 \, \mathrm{d}u + \alpha \int_{u=t_1}^{\infty} G_2 \, \mathrm{d}u. \tag{17}$$

Here t_1 is the partitioning time, G_2 is the usual series-form of the transient GF, and function G_1 is an alternate form with better convergence behavior when u is small.

The alternate GF, G_1, depends on the specific boundary conditions involved. Since we are interested primarily in temperatures caused by a specified heating at the $z = 0$ surface, we

Table 4. Eigenfunction, norm, and eigenvalues along the z-direction. Note $B_1 = h_1 L/k$; $B_2 = h_2 L/k$.

(a) Eigenfunctions

Cases	$Z_\ell(z)$
Z11, Z12, and Z13	$\sin(\lambda_\ell z)$
Z21, Z22, and Z23	$\cos(\lambda_\ell z)$
Z31, Z32, and Z33	$\lambda_\ell L \cos(\lambda_\ell z) + B_1 \sin(\lambda_\ell z)$

(b) Inverse norm and eigenvalues or conditions

Case	$N_z(\ell)^{-1}$	λ_ℓ or eigencondition
Z11	$2/L$	$\ell\pi/L$
Z12	$2/L$	$\frac{(2\ell-1)\pi}{2L}$
Z13[a]	$2\phi_\ell/L$	$\lambda_\ell L \cot(\lambda_\ell L) = -B_2$
Z21	$2/L$	$\frac{(2\ell-1)\pi}{2L}$
Z22	$2/L;\ \lambda_\ell \neq 0$ $1/L;\ \lambda_\ell = 0$	$\ell\pi/L$
Z23[a]	$2\phi_\ell/L$	$\lambda_\ell L \tan(\lambda_\ell L) = B_2$
Z31	$\frac{2}{(\lambda_\ell L)^2+B_1^2+B_1}$	$\lambda_\ell L \cot(\lambda_\ell L) = -B_1$
Z32	$\frac{2}{(\lambda_\ell L)^2+B_1^2+B_1}$	$\lambda_\ell L \tan(\lambda_\ell L) = B_1$
Z33[b]	$2\Phi_\ell/L$	$\tan(\lambda_\ell L) = \frac{\lambda_\ell L(B_1+B_2)}{(\lambda_\ell L)^2 - B_1 B_2}$

[a] $\phi_\ell = [(\lambda_\ell L)^2 + B_2^2]/[(\lambda_\ell L)^2 + B_2^2 + B_2]$
[b] $\Phi_\ell = \phi_\ell \div [(\lambda_\ell L)^2 + B_1^2 + B_1\phi_\ell]$

will limit the discussion to type 2 boundaries at $z = 0$. Further, as the transient GF involves a product of lower-dimensional GF, the discussion need only consider the z-direction portion of the triple-sum GF.

Consider the following expression for a one-dimensional transient GF in the z-direction:

$$G_z(z, z' = 0, u) = \frac{2}{\sqrt{4\pi\alpha u}} \exp\left[-\frac{z^2}{4\alpha u}\right]. \tag{18}$$

This expression exactly describes heat conduction into a semi-infinite body with heating at the $z' = 0$ surface, but it is also accurate in a finite body ($0 < z < L$) for u small (accuracy is six significant figures for $\alpha u/L^2 < 0{\cdot}05$ and for z near zero), and the level of approximation improves for smaller values of u.

To construct function G_1, multiply the above approximate z-direction term by the portion that depends on (r, ϕ), Equation (13). Then

$$G_1(r, \phi, z, r', \phi', z' = 0, u) \;=\; \sum_{n=0}^{\infty}\sum_{m=1}^{\infty} \frac{R_{nm}(r) R_{nm}(r')}{N_r(nm)} \; \frac{\cos[n(\phi - \phi')]}{N_\phi(n)} \tag{19}$$

$$\times \ \exp\left[-\beta_{nm}^2 \alpha u\right] \ \frac{2}{\sqrt{4\pi\alpha u}} \exp\left[-\frac{z^2}{4\alpha u}\right].$$

The above expression has been limited to cases $R0I\Phi00Z2J$ where I, J =1 or 3 only in the interest of brevity (note that the $m = 0$ and $\ell = 0$ terms are missing.) Now, to evaluate the time-partitioned form of the GF, substitute the above expression for G_1 and the product of Equation (13) and (14) for G_2 in the time integrals given in Equation (17). The result, evaluated at $z = 0$, is given by:

$$G(r, \phi, 0\,|r', \phi', 0) \ = \ \sum_{n=0}^{\infty}\sum_{m=1}^{\infty} \frac{R_{nm}(r)R_{nm}(r')}{N_r(nm)} \ \frac{\cos[n(\phi-\phi')]}{N_\phi(n)} \tag{20}$$
$$\times \ \left\{ \frac{1}{\beta_{nm}} \operatorname{erf}\left[\beta_{nm}\sqrt{\alpha t_1}\right] + \sum_{\ell=1}^{\infty} \frac{\exp[-(\beta_{nm}^2+\lambda_\ell^2)\alpha t_1]}{(\beta_{nm}^2+\lambda_\ell^2)} \ \frac{1}{N_z(\ell)} \right\}.$$

For a derivation of the above expression, and results for $z \neq 0$, refer to Appendix B. The above form of the GF, constructed with time-partitioning, has improved convergence properties because the triple-sum portion of the series contains an exponential term which goes quickly to zero as the eigenvalues increase (with increasing n or m). The error function term also contributes to the convergence of the double-sum portion of the series. A side benefit of time partitioning is an additional error-checking technique. Since the results should be independent of the partition time, by varying the partition time a good check can be made on the numerical values computed from this expression. Again, the above expression does not include any case described by numbers R02 or Z22 (for these the $m = 0$ and $\ell = 0$ terms are needed).

7. Influence functions

One application for the GF is construction of influence functions for boundary-element methods. The influence function is found by integrating the GF over a portion of the body surface (the boundary-element itself). The influence function is an important numerical tool because it may be evaluated anywhere in the body, since the singularity in the GF is completely removed by integration [5, p. 117]. Also, the process of integration improves the series convergence compared to that for the GF itself.

7.1. Element on a flat boundary ($z = 0$)

For a boundary-element located on a flat boundary of the cylinder, the natural shape of the boundary-element is a finite arc ($r_1 < r < r_2$; $\phi_1 < \phi < \phi_2$). The discussion below focuses on boundary $z = 0$ of the cylinder, and the corresponding element located at the $z = L$ boundary (not shown) may be similarly obtained. The influence function at $z = 0$ is given by

$$\psi = \int_{r_1}^{r_2} \int_{\phi'=\phi_1}^{\phi_2} G_{z'=0} \, r' \mathrm{d}\phi' \mathrm{d}r'. \tag{21}$$

The required integral on ϕ' is given by:

$$\int_{\phi'=\phi_1}^{\phi_2} \cos[n(\phi-\phi')]\mathrm{d}\phi' = \{\sin[n(\phi-\phi_1)] - \sin[n(\phi-\phi_2)]\}/n. \tag{22}$$

The required integral on r' is given by

$$\int_{r_1}^{r_2} J_n(\beta_{nm} r')\, r' \mathrm{d}r' \tag{23}$$

This integral was evaluated numerically with the trapezoidal rule and with precision controlled by a Romberg scheme [16].

7.2. Element on the curved boundary $r = a$

When the boundary-element is located on the curved boundary of the cylinder the required integration takes place over the region ($z_1 < z < z_2$; $\phi_1 < \phi < \phi_2$). The influence function at $r = a$ is given by

$$\psi = \int_{z_1}^{z_2} \int_{\phi'=\phi_1}^{\phi_2} G_{r'=a}\, a\, \mathrm{d}\phi' \mathrm{d}z' \tag{24}$$

The ϕ'-integral has already been given above in Equation (22). The integral needed over z' falls on the kernel function for the double-sum GF:

$$\int_{z_1}^{z_2} P_{nm}(z, z')\, \mathrm{d}z' \tag{25}$$

This integral can be carried out easily on the exponentials which appear in Equation (7).

8. Numerical example

In this section numerical values for an influence function are given. The specific geometry is case R03Φ00Z23 with the surface element located on the $z = 0$ surface of the cylinder. All of the numerical results discussed in this section were found from the double-sum GF integrated over a portion of the $z' = 0$ surface.

The application for this geometry is a thermal sensor. The sensor consists of a small metal film plated on a portion of the flat face of a button-shaped cylinder of quartz, about 6 mm in diameter. The quartz cylinder is flush-mounted in the wing of an aircraft with the plated metal film exposed to the flowing air. The metal film, when operated with a 'constant temperature' bridge circuit (which actually maintains a fixed electric resistance by controlling the electric current), may be calibrated to provide information on the air flow over the wing. The author has previously published boundary-element results for the thermal behavior of this sensor, but with a semi-infinite region to represent the quartz substrate [17]. The present numerical example provides an improved geometric description of the quartz substrate. (A complete thermal model of this sensor also involves an influence function for the flowing air, beyond the scope of this paper.)

Consider a cylinder with aspect ratio $a/L = 1$ that is uniformly heated over the half-circle $0 < r/a < 0{\cdot}5$ and $-\pi/2 < \phi < \pi/2$, and the remainder of the $z = 0$ surface is insulated. The $r = a$ and $z = L$ surfaces of the cylinder are exposed to a heat sink with contact conductance described by Biot number $B_i = hL/k$. Figure 1 shows a contour plot of the normalized surface temperature, $(T - T_\infty)/(q_0 a/k)$, where q_0 is the heat flux and T_∞ is the temperature of the surroundings. Only half the $z = 0$ surface is shown since the temperature is symmetric about $\phi = 0$. In Figure 1 the Biot number has the large value $B_i = 10$ so that

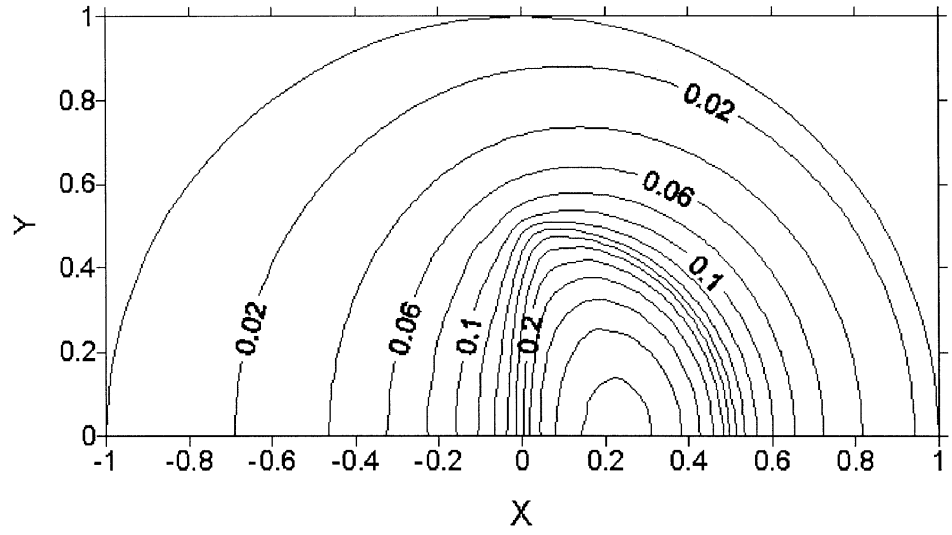

Figure 1. Contours of normalized temperature on the $z = 0$ face of the cylinder heated over a half-circle $r < a/2$. Convection on other surfaces of the cylinder are described by Biot = 10.

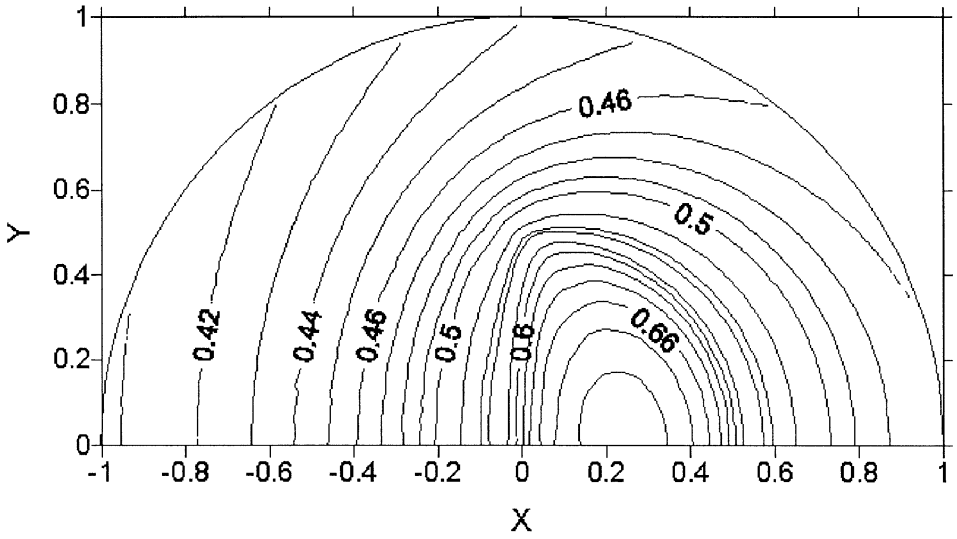

Figure 2. Contours of normalized temperature on the $z = 0$ face of the cylinder heated over a half-circle $r < a/2$. Convection on the other surfaces of the cylinder are described by Biot = 0·10.

the (normalized) temperature at the outer diameter of the cylinder is nearly zero. In Figure 2 the same heating conditions are shown but now the Biot number has the small value $B_i = 0{\cdot}1$. Consequently in Figure 2 the peak temperatures are higher and the outer boundary of the cylinder has a clearly-defined distribution of temperature.

As another example, Figure 3 shows the temperature caused by a smaller heated region $0{\cdot}4 < r/a < 0{\cdot}5$ and $-1 < \phi < +1$. In this case the Biot number is $B_i = 1{\cdot}0$. Note that the peak temperature is smaller than before, in part because there is less heat energy introduced over a smaller heated region (temperature is normalized by heat flux, not energy). The temperature gradients near the heated region are much steeper, however. Boundary elements of any shape bounded by $r =$ constant or $\phi =$ constant are easily constructed with this

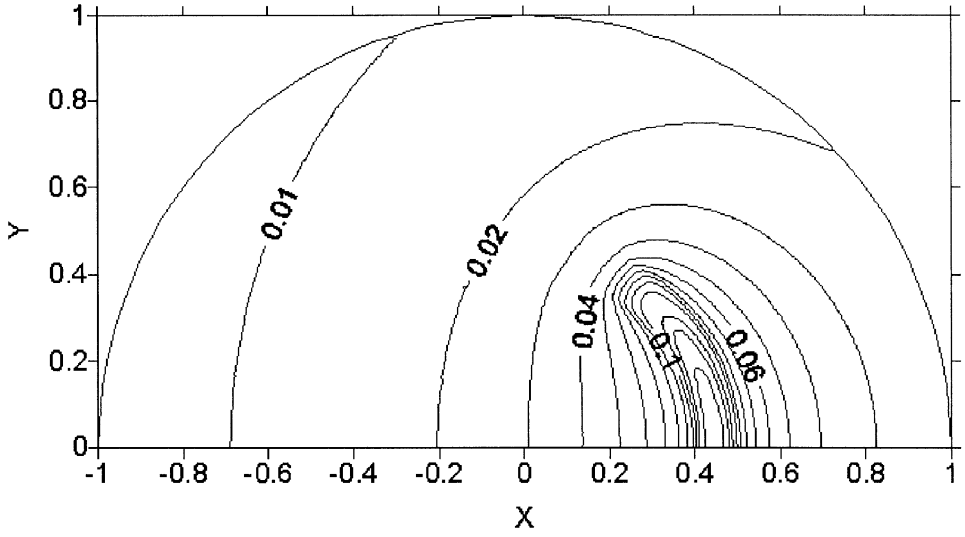

Figure 3. Contours of normalized temperature on the $z = 0$ face of the cylinder heated over $0 \cdot 4 < r/a < 0 \cdot 5$ and $-1 < \phi < 1$. Convection on the other surfaces of the cylinder are described by Biot $= 1$.

code. Although surface temperatures (at $z = 0$) are of primary interest for the thermal-sensor problem, temperatures inside the cylinder ($0 < z < L$) may be computed with the same code.

Figures 1 and 2 were each constructed from 4000 individual temperature values; about 175 CPU seconds were required to compute the temperatures for each figure. Figure 3 was constructed from 62,000 individual temperature values which required proportionately more computer time. The influence function was coded in double-precision Fortran 77 and run under the Solaris operating system on a Sun Blade 2000 with dual 900 MHz processors.

Whenever infinite series are used to compute numerical values, the convergence properties of the series control whether the task is easy or difficult. For this work the double-sum series was evaluated beginning with $n = 0$, and then terms of the m-series were added until the sum of the last five terms, divided by the total sum so far, was less than a tolerance. The use of five terms together is important because of the sinusoidal-like oscillation of the Bessel function. Additional m-series for $n = 1$, $n = 2$ and so on are then added. The series was truncated when the sum of the last three n-terms (each composed of a converged m-series), divided by the total sum so far, was less than a chosen tolerance. For Figures 1, 2, and 3 the tolerance used was 10^{-5}.

Several values of the convergence tolerance were investigated for their effect on the double-sum form. Table 5 shows several (normalized) temperature values, and the number of series terms required to compute them, with convergence tolerance values 10^{-4}, 10^{-5}, and 10^{-6}, and for Biot $= 1$. The temperature values changed slightly as the tolerance decreases, and as expected the number of series terms required increases. Note that fewer terms in the series are required inside the cylinder ($0 < z < L$) where the exponential terms have negative arguments that improve the convergence. The slowest convergence occurs at the ends of the cylinder ($z = 0$ and $z = L$) where some of the exponential terms have a zero argument. The ultimate accuracy of the calculation is probably limited by the accuracy of the routine for Bessel function J_n, especially at moderate order n for which a recursion technique is used [16]. At large order n an accurate asymptotic relation is available.

Table 5. Number of terms required for computing temperature in the cylinder with varying convergence tolerance. Surface $z = 0$ is heated over a half circle with $r = a/2$, similar to Figures 1 and 2, but with Biot = 1.

Tolerance	x/a	y/a	z/L	$(T - T_\infty)/(q_0 a/k)$	terms
10^{-4}	0·2	0·2	0·0	0·3157740	285
	0·4	0·4	0·0	0·1594807	315
	0·6	0·6	0·0	0·0862996	250
	0·2	0·2	0·4	0·1140853	60
	0·4	0·4	0·4	0·0937014	65
	0·6	0·6	0·4	0·0686602	65
	0·2	0·2	0·8	0·0608919	60
	0·4	0·4	0·8	0·0548472	60
	0·6	0·6	0·8	0·0448605	60
10^{-5}	0·2	0·2	0·0	0·3149307	665
	0·4	0·4	0·0	0·1595780	635
	0·6	0·6	0·0	0·0863836	640
	0·2	0·2	0·4	0·1140853	75
	0·4	0·4	0·4	0·0937021	90
	0·6	0·6	0·4	0·0686604	95
	0·2	0·2	0·8	0·0608919	60
	0·4	0·4	0·8	0·0548472	65
	0·6	0·6	0·8	0·0448605	65
10^{-6}	0·2	0·2	0·0	0·3148189	1325
	0·4	0·4	0·0	0·1595351	2630
	0·6	0·6	0·0	0·0863894	1295
	0·2	0·2	0·4	0·1140853	95
	0·4	0·4	0·4	0·0937020	115
	0·6	0·6	0·4	0·0686604	115
	0·2	0·2	0·8	0·0608919	65
	0·4	0·4	0·8	0·0548472	65
	0·6	0·6	0·8	0·0448605	65

Computing the eigenvalues consumed a large component of the computer time required for the calculation. To speed up the calculations for one graph, the eigenvalues were stored and re-used for subsequent temperature values. This is possible because the eigenvalues change only when the Biot number changes or when the aspect ratio of the cylinder changes. Eigenvalues were computed sequentially, beginning with $n = 0$ and $m = 1$. For each value of n and m, a new eigenvalue was computed only if no eigenvalue had been previously stored.

9. Conclusion

In this paper three series expressions are given for steady three-dimensional GF in the cylinder including a classic triple sum series based on eigenfunction expansions and a double-sum

series based on kernel functions. The double-sum series generally has better convergence properties than the classic triple-sum series. All combinations of boundary conditions of type 1, 2 and 3 are treated.

A new triple-sum form is constructed with the method of time partitioning, which the author has previously applied to solutions in the Cartesian coordinate system. Time partitioning is a general method for improving the series convergence of both steady and unsteady heat conduction solutions.

A numerical example is given for a cylinder with boundary conditions of type 2 and 3 and results are presented in the form of an influence function. Specifically, the influence function is the temperature in the cylinder caused by uniform heating over a small portion of the surface, in this case at $z = 0$. The double-sum form of the series solution was used to compute the influence function throughout the cylinder. The slowest numerical convergence of the influence function occurs at locations $z = 0$ and $z = L$. Futher work is needed to improve the convergence at these points where the exponential terms in the kernel functions do not assist the convergence as they do for locations inside the cylinder.

Influence functions are an important part of boundary-element calculations. A specific application of the present work is a boundary-element simulation of the cylindrical substrate of a flush-mounted hot-film sensor. In future work, a complete thermal simulation of this a sensor could be carried out by including additional influence functions for the temperature in air flowing over a heated surface. Flush-mounted hot-film sensors may be used in very high speed flows, in which a traditional protruding sensor (such as a pitot tube) would be burned away. Hot-film sensors have been used by NASA on the Pegasus air-launched used as a first stage for hypersonic flight tests.

Acknowledgements

The author is grateful to David H. Y. Yen of Michigan State University for his correspondence and suggestions regarding this work.

Appendix A. Modified GF for Neumann boundaries

In this appendix the special case of type 2 (Neumann) conditions on all boundaries is treated. Although the temperature problem for this case may have a non-trivial solution, the Green's function defined by Equation (3) does not exist. Following Barton [5], a modified GF, denoted G_m, may be defined that satisfies

$$\nabla^2 G_m = -\frac{1}{r}\delta(r - r')\delta(\phi - \phi')\delta(z - z') + \frac{1}{V}, \tag{A1}$$

where

$$\nabla^2 G_m = \left(\frac{\partial^2}{\partial r^2} + \frac{1}{r}\frac{\partial}{\partial r} + \frac{1}{r^2}\frac{\partial^2}{\partial \phi^2} + \frac{\partial^2}{\partial z^2}\right) G_m$$

and where $V = \pi a^2 L$ is the volume of the cylinder. Physically, the term $1/V$ is a uniformly distributed heat sink to remove the heat introduced by the point source at (r', ϕ', z'). Since no heat passes through homogeneous boundaries of type 2 (insulated), without this term the

differential equation cannot be satisfied. It is proposed that the modified GF has the form

$$\begin{aligned} G_m(r,\phi,z|r',\phi',z') &= \frac{R_{00}(r)R_{00}(r')}{N_r(00)}\frac{1}{N_\phi(0)}P_{00}(z,z') \\ &+ \sum_{m=1}^{\infty}\frac{R_{0m}(r)R_{0m}(r')}{N_r(0m)}\frac{1}{N_\phi(0)}P_{0m}(z,z') \\ &+ \sum_{n=1}^{\infty}\sum_{m=1}^{\infty}\frac{R_{nm}(r)R_{nm}(r')}{N_r(nm)}\frac{cos[n(\phi-\phi')]}{N_\phi(n)}P_{nm}(z,z'). \end{aligned} \tag{A2}$$

Here kernel function P_{00} satisfies a modified differential equation:

$$\frac{\mathrm{d}^2P_{00}}{\mathrm{d}z^2} = -\delta(z-z') + \frac{1}{L} \tag{A3}$$

A proof that G_m satisfies the differential equation, prepared by D.H.Y. Yen, is available from the author [18].

The modified Green's function G_m may be used to find the temperature with the Green's function-solution equation, Equation (2), with the following additional constraints: the sum of the heat passing through the boundaries must be equal to the total amount of heat introduced by volume energy generation g; and, since the spatial average temperature of the body computed from G_m is zero, the average temperature in the body must be supplied as part of the input data to the problem.

Appendix B. Integrals in time-partitioning

In this appendix two integrals that appear in the time-partitioned form of the GF will be given in closed form.

B.1. SMALL-TIME INTEGRAL

Consider first the integral

$$\alpha\int_{u=0}^{t_1} G_1\,\mathrm{d}u, \tag{B1}$$

where G_1 is given by Equation (19). The u-varying portion of this integral is given by:

$$I_1 = \alpha\int_{u=0}^{t_1}\exp\left[-\beta_{nm}^2\alpha u\right]\frac{2}{\sqrt{4\pi\alpha u}}\exp\left[-\frac{z^2}{4\alpha u}\right]\mathrm{d}u \tag{B2}$$

This integral may be evaluated with the following identity [8, p. 428]:

$$\int x^{-1/2}\,\mathrm{e}^{-a^2x-b^2/x}\mathrm{d}x = \frac{\sqrt{\pi}}{2a}\left\{\mathrm{e}^{2ab}\,\mathrm{erf}\left[a\sqrt{x}+\frac{b}{\sqrt{x}}\right]+\mathrm{e}^{-2ab}\,\mathrm{erf}\left[a\sqrt{x}-\frac{b}{\sqrt{x}}\right]\right\}, \tag{B3}$$

where erf is the error function. Let $a^2 = \beta_{nm}^2\alpha$ and $b^2 = z^2/(4\alpha)$, and using $\mathrm{erf}(\pm\infty) = \pm1$, the u-varying portion of the integral on G_1 is given by:

$$I_1 = \frac{1}{2\beta_{nm}}\left\{\mathrm{e}^{\beta_{nm}z}\,\mathrm{erf}\left[\beta_{nm}\sqrt{\alpha t_1}+\frac{z}{\sqrt{4\alpha t_1}}\right]+\mathrm{e}^{-\beta_{nm}z}\,\mathrm{erf}\left[\beta_{nm}\sqrt{\alpha t_1}-\frac{z}{\sqrt{4\alpha t_1}}\right]\right\}. \tag{B4}$$

B.2. LARGE-TIME INTEGRAL

The large-time integral needed has the form

$$\alpha \int_{u=t_1}^{\infty} G_2 \, \mathrm{d}u \tag{B5}$$

where G_2 is the triple-sum form of the GF given by Equation (15). The portion of G_2 that depends on time variable u has the form of an exponential, in the form

$$I_2 = \alpha \int_{u=t_1}^{\infty} \exp\left[-\beta_{nm}^2 \alpha u\right] \, \exp\left[-\lambda_\ell^2 \alpha u\right] \mathrm{d}u. \tag{B6}$$

This integral may be evaluated to give

$$I_2 = \frac{\exp[-(\beta_{nm}^2 + \lambda_\ell^2)\alpha t_1]}{(\beta_{nm}^2 + \lambda_\ell^2)} \tag{B7}$$

Time partitioning is important because this exponential term goes to zero rapidly as n, m, and ℓ become large in the triple sum. In contrast, consider the above expression with no time partitioning, for which $t_1 \to 0$. In this case $I_2 = 1/(\beta_{nm}^2 + \lambda_\ell^2)$. Although this term is mathematically convergent, it can require many thousands of terms for six-digit precision.

References

1. P.M. Morse and H. Feshbach, *Methods of Theoretical Physics.* New York: McGraw-Hill (1953) 997 pp.
2. H.S. Carslaw and J.C. Jaeger, *Conduction of Heat in Solids.* Oxford: Oxford University Press (1959) 510 pp.
3. I. Stakgold, *Boundary Value Problems of Mathematical Physics, Vol. 1.* New York: Macmillan (1967) 340 pp.
4. D.G. Duffy, *Green's Functions with Applications.* Boca Raton, FL: Chapman and Hall (2001) 443 pp.
5. G. Barton, *Elements of Green's Functions and Propagation.* Oxford: Oxford University Press (1989) 523 pp.
6. A.G. Butkovskii, *Green's Functions and Transfer Functions Handbook.* New York: Halsted Press (division of Wiley) (1982) 236 pp.
7. A.G. Butkovskii and L.M. Pustyl'nikov, *Characteristics of Distributed-Parameter Systems.* Dordrecht: Kluwer (1993) 412 pp.
8. J.V. Beck, K.D. Cole, A. Haji-Sheikh, and B. Litkouhi, *Heat Conduction Using Green's Functions.* New York: Hemisphere Publishing (1992) 523 pp.
9. I.M. Dolgova, and Y.A. Melnikov, Construction of Green's functions and matrices for equations and systems of the elliptic type. *J. Appl. Math. Mech.* 42 (1978) 740–746.
10. Y.A. Melnikov, *Green's Functions in Applied Mechanics.* Boston: Computational Mechanics Publications (1995) 267 pp.
11. Y.A. Melnikov, *Influence Functions and Matrices.* New York: Marcel Dekker (1999) 469 pp.
12. K.D. Cole and D.H.Y. Yen, Green's functions, temperature, and heat flux in the rectangle. *Int. J. Heat Mass Transfer* 44 (2001) 3883–3894.
13. K.D. Cole and D.H.Y. Yen, Influence functions for the infinite and semi-infinite strip. *J. Thermophys. Heat Transfer* 15 (2001) 431–438.
14. P.E. Crittenden and K.D. Cole, Fast-converging steady-state heat conduction in the rectangular parallelepiped. *Int. J. Heat Mass Transfer* 45 (2002) 3585–3596.
15. D.H.Y. Yen, J.V. Beck, R.L. McMasters, and D. Amos, Solution of an initial-boundary-value problem for heat conduction in a parallelepiped by time partitioning. *Int. J. Heat Mass Transfer* 45 (2002) 4267–4279.
16. W.H. Press, *et al.*, *Numerical Recipes.* Cambridge: Cambridge University Press (1992) 963 pp.
17. P.W. Liang and K.D. Cole, Transient conjugate heat transfer from a rectangular hot film. *J. Thermophys. Heat Transfer* (1992) 349–355.
18. D.H.Y. Yen, personal communication (2003).